EURRAD 00409

Image segmentation: methods and applications in diagnostic radiology and nuclear medicine

P. Suetens*[,a], E. Bellon[a], D. Vandermeulen[a], M. Smet[a], G. Marchal[a], J. Nuyts[b], L. Mortelmans[b]

[a]*Interdisciplinary Research Unit for Radiological Imaging, Department of Electrical Engineering and Department of Radiology, ESAT, Kardinaal Mercierlaan 94, B-3001 Heverlee, Belgium,* [b]*Department of Nuclear Medicine, Katholieke Universiteit, Leuven, Belgium*

Abstract

We review and discuss different classes of image segmentation methods. The usefulness of these methods is illustrated by a number of clinical cases. Segmentation is the process of assigning labels to pixels in 2D images or voxels in 3D images. Typically the effect is that the image is split up into segments, also called regions or areas. In medical imaging it is essential for quantification of outlined structures and for 3D visualization of relevant image data. Based on the level of implemented model knowledge we have classified these methods into (1) manual delineation, (2) low-level segmentation, and (3) model-based segmentation. Pure manual delineation of structures in a series of images is time-consuming and user-dependent and should therefore be restricted to quick experiments. Low-level segmentation analyzes the image locally at each pixel in the image and is practically limited to high-contrast images. Model-based segmentation uses knowledge of object structure such as global shape or semantic context. It typically requires an initialization, for example in the form of a rough approximation of the contour to be found. In practice it turns out that the use of high-level knowledge, e.g. anatomical knowledge, in the segmentation algorithm is quite complicated. Generally, the number of clinical applications decreases with the level and extent of prior knowledge needed by the segmentation algorithm. Most problems of segmentation inaccuracies can be overcome by human interaction. Promising segmentation methods for complex images are therefore user-guided and thus semi-automatic. They require manual intervention and guidance and consist of fast and accurate refinement techniques to assist the human operator.

Key words: Images, processing; Images, analysis; Images, quality; PACS; Computers in radiology; Departmental management

1. Introduction

Segmentation is the process of assigning labels to pixels in 2D images or voxels in 3D images. Typically the effect is that the image is split up into segments, also called regions or areas. Segmentation in medical imaging is essential for quantification of outlined structures and for 3D visualization of relevant image data.

Methods for image segmentation can be classified into two subgroups low-level segmentation and model-based segmentation. Low-level segmentation represents by far the majority of clinically used methods. They rely entirely on image operators that analyze local photometry or local shape in the image. Finding bony structures in CT images based on homogeneity of the intensity values is an example. Model-based segmentation methods exploit knowledge of object structure such as global shape or semantic context. Examples are the detection of circular lung nodules in X-rays and the use of an anatomy atlas for segmentation of MR images of the brain.

*Corresponding author.

We note that segmentation errors due to an incomplete model are often unavoidable. This is partly due to our limited capability of explicitly describing our knowledge of the structures to be segmented. Furthermore, the use of a more complete model may still require unrealistically high computational power for clinical practice. User interaction may therefore be necessary to correct segmentation errors. For some small experiments it may even be recommended to do the complete segmentation task manually.

We now describe and illustrate different methods for image segmentation. Based on the level of implemented model knowledge we have classified these methods into (1) manual delineation, (2) low-level segmentation and (3) model-based segmentation.

2. Methods and applications

2.1. Manual delineation

Pure manual delineation of structures in a series of images is time-consuming. However, it may be most

suited for quick experiments or measurements on a limited number of cases, which otherwise would require important modifications to existing segmentation software. As explained below in the section on model-based segmentation, manual delineation may also be needed as a rough indication of the position of the contour, which is then further optimized by the segmentation program. As compared to pure manual delineation the spatial accuracy of this approximate contour is less important.

Manual or semi-automatic outlining methods require quite sophisticated human–computer interfaces. The software must combine the capabilities of drawing programs, which are well-known from the area of personal computers, and the features of a radiological display system. For example, it must be possible to draw and modify flexible curves, which are superimposed onto the image, as well as to zoom the image during this task. Since radiological image data typically consist of many image slices with a large range of gray values, options must be available for gray value windowing and for navigating through the images, such as interactive cine mode. It can then for example be useful to transfer a contour that has been drawn on a previous slice.

Figure 1a shows a reformatted sagittal slice of a spiral CT scan in which the diaphragm was manually outlined. Note that the diaphragm is hardly visible near the heart, which would increase the complexity of an automatic segmentation method. This process was repeated for consecutive slices and the resulting surface was displayed three dimensionally (Fig. 1b). The surface-based representation gives insight into the global shape of the diaphragm, particularly into the relation between the shape at inspiration and expiration.

Figure 2 shows a gated MR image of the heart obtained with cardiac tagging by selectively saturating tissue along well-chosen planes. The tags are used to follow different points of the heart during the heart cycle for further quantification of the left ventricular myocardial function. The manual outlining was done by fitting a smooth curve through the limited number of points the user entered. The use of splines is a widespread method for such smoothing.

Fig. 1. (a) Reformatted sagittal slice of a spiral CT scan with manual delineation of the diaphragm. (b) Surface-based representation of the diaphragm obtained from 25 consecutive sagittal CT slices. (Courtesy J. Verschakelen and J. Bogaert).

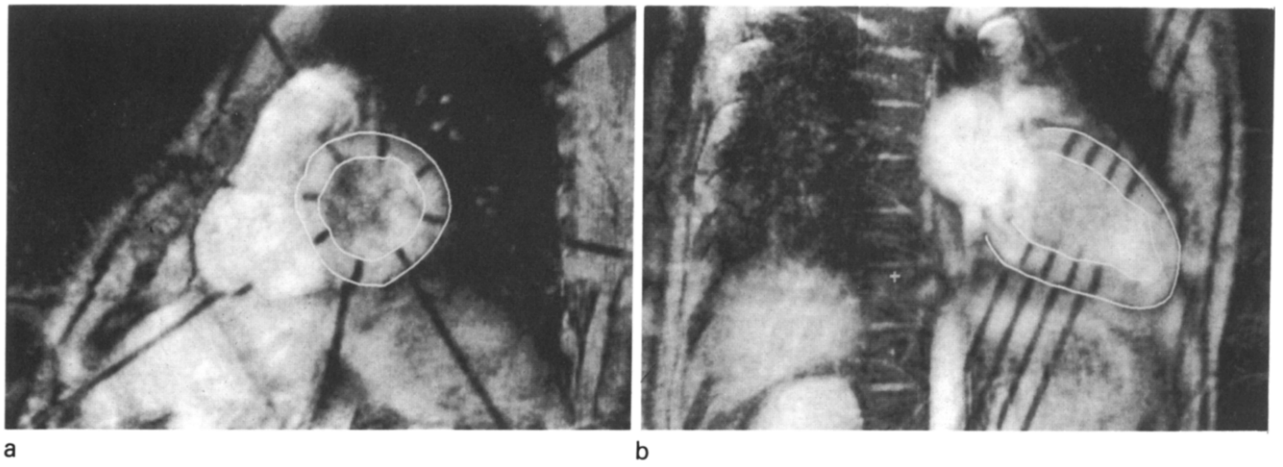

Fig. 2. Gated MR image of the heart obtained with cardiac tagging. (a) Short axis view. (b) Long axis-view corresponding to one of the tag planes in part a. (Courtesy J. Bogaert and F. Rademakers).

2.2. Low-level segmentation

Low-level segmentation methods rely entirely on image operators that analyze the intensity, texture or shape locally at each pixel in the image. Since the knowledge of the structures to be segmented must be expressed in terms of local characteristics, it can be expected that the performance of low-level segmentation is limited and that user interaction is often needed to correct the result.

The simplest method is a threshold operation applied to the original gray values of the images. The pixels are then labeled as either object or background pixels. This method works relatively well for high-contrast images, such as CT images of bony structures. In some cases it may be necessary to combine the selected object or foreground pixels into groups of adjacent points. Figure 3 shows such an example, obtained from a series of spiral CT images. It is a shaded representation of the cervical vertebrae of a patient with extreme arthrosis of the cervical facet joints. Figure 3a is the result of simple thresholding, while Fig. 3b was obtained by grouping adjacent foreground pixels, starting from a seed pixel selected by the user. The same image acquisition, segmentation and display method was used to obtain the image of Fig. 4, which shows a bilateral compression of the trachea of a patient with enlarged thyroid gland.

Combining neighboring pixels with similar local characteristics is also called region growing. We note that, instead of gray value similarity, other local image features, such as texture or the intensity gradient, may also be used as the grouping criterion. Grouping of high intensity gradients is a possible edge detection method. An edge follower or tracker is then used to combine edge pixels into long edges, such as contours. However, due to the heuristic nature of edge tracking, a suitable result cannot be guaranteed and the clinical usefulness is therefore limited.

In practice different regions may touch via one or more thin interconnecting branches. Manual interaction can simply separate these regions. The number of user interventions can strongly be reduced if an opening, i.e. an erosion followed by a dilation, is applied. Erosion removes spikes from the edges of the regions, while dilation restores the original size of the regions without the spikes. Figures 5 and 6 are examples. Figure 5b is an image of the common carotid arteries and their internal and external branches, obtained from a spiral CT scan. Compare with Fig. 5a, which shows that arteries and veins cannot be separated by nonselective thresholding. Figure 6 is a surface-based representation of the brain obtained from MRI. Note the communication between the occipital horn of the lateral ventricular and subarachnoidal space.

The above opening and closing operations are examples of binary morphological operations. A more complex case of morphological gray value filtering is the line detector that we developed for finding blood vessels in magnetic resonance angiography (MRA). An angiographic image is traditionally obtained by a maximum intensity projection (MIP) (Fig. 7a). However, small blood vessels may be obscured by non-vascular areas of high intensity, and 'black vessels' are not visible in a MIP. 'Black vessels' are vessels with turbulent flow yielding low signal, such as near a stenosis or an aneurysm or in the feeding artery of an AVM or a tumor. They can be detected (Fig. 7b) by the following morphological filter.

(1) A MIP of a cubic environment of a central voxel is made in the three main directions. Only the projection with the largest mean gray value is retained. In the case of a blood vessel this projection is a long-axis view.

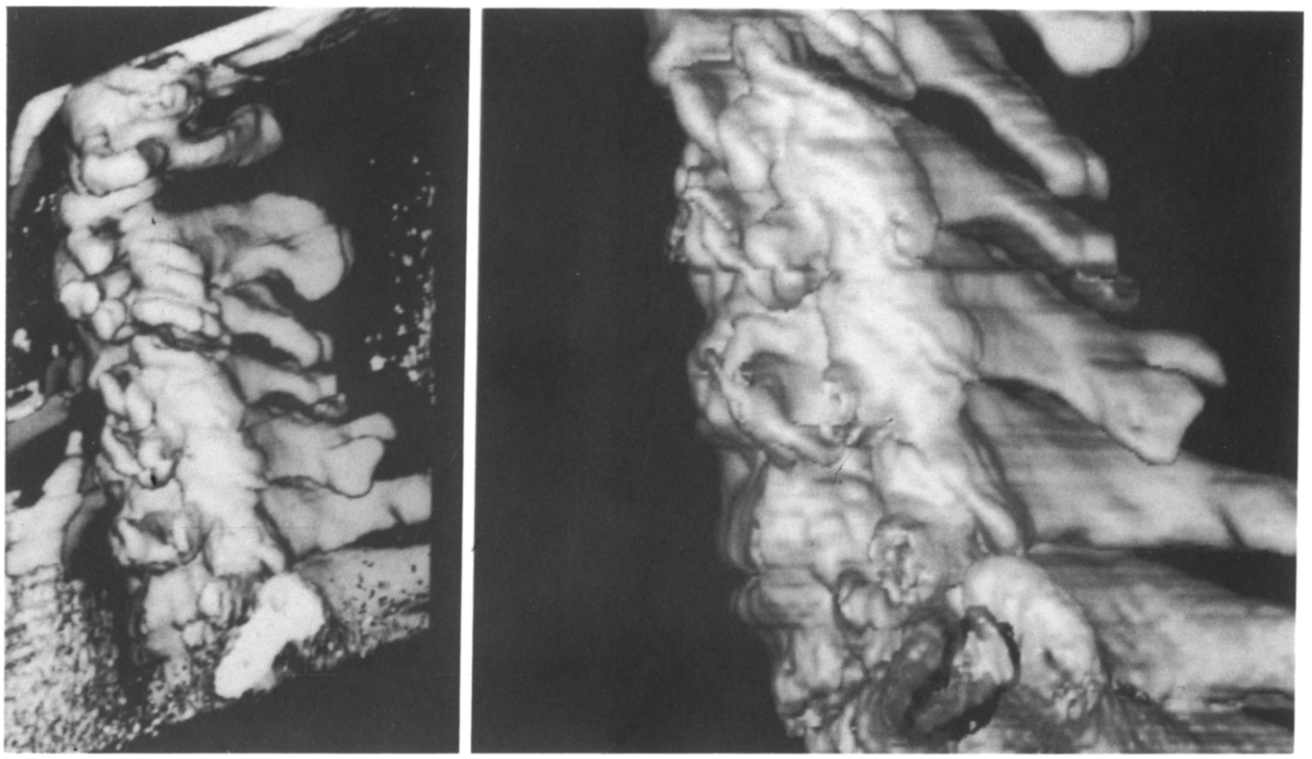

Fig. 3. (a) Shaded representation of the cervical vertebrae of a patient with extreme arthrosis of the cervical facet joints, segmented by simply thresholding a series of 127 spiral CT images of 2 mm thickness and slice distance of 1 mm. (b) Same as part a, but obtained by region growing.

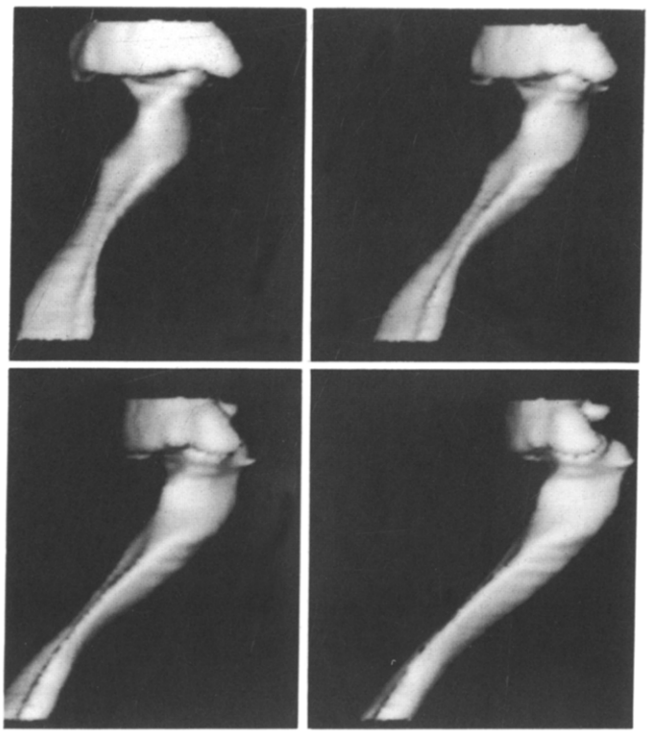

Fig. 4. Shaded representation of a bilateral compression of the trachea of a patient with enlarged thyroid gland, segmented by region growing. (Courtesy J. Bogaert and J. Verschakelen).

(2) Starting from the central pixel in the projection (this is the projection of the central voxel of the 3D environment) the minimal intensity pixel in eight directions is searched for. The directions of the two largest of these eight minima subdivide the projection plane into two halfplanes. In the case of a blood vessel these halfplanes correspond to both sides of the vessel trajectory.

(3) In both halfplanes, the minimal intensity pixel is searched for. The largest gray value of both minima is finally subtracted from the intensity of the original voxel.

The most important property of this filter is that 2D (plane) and 3D (volumetric) structures with high intensity are suppressed because they completely fill the projection plane of the local MIP. Line structures (1D) on the other hand are not affected. The contrast between vessels and tissue is thus enhanced. Noise pixels are not affected either. Note that the result of this morphological operator is a new gray value image, in which the gray values must be considered as a measure of belief that the corresponding point belongs to a line like structure. More details can be found in [1,2].

2.3. Model-based segmentation

Model-based methods use knowledge of object structure, such as global shape or semantic context, thus

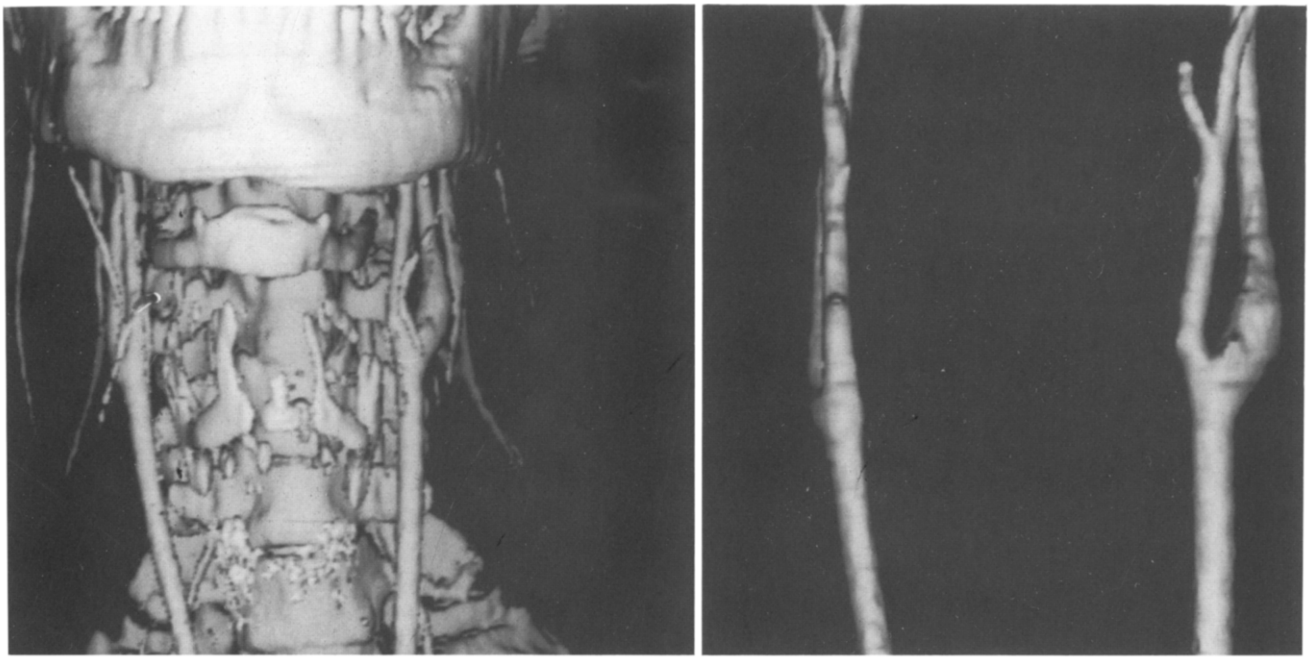

a b

Fig. 5. (a) Shaded representation of arteries and veins segmented by simply thresholding a series of spiral CT images with slice thickness of 5 mm and slice distance of 1 mm. (b) Common carotid arteries and their internal and external branches, obtained by region growing and a morphological opening operation applied to the same image data as part a.

distinguishing them from the low-level methods, which exploit only local gray value statistics or local shape. Knowledge of global shape or semantic context may assist the segmentation process in cases of poor resolution, noise and low contrast. The model instance that best fits the image data can then be found by means of a mathematical optimization approach. Among the possible optimization procedures are dynamic programming, solving differential equations, and relaxation. An example of each is given below.

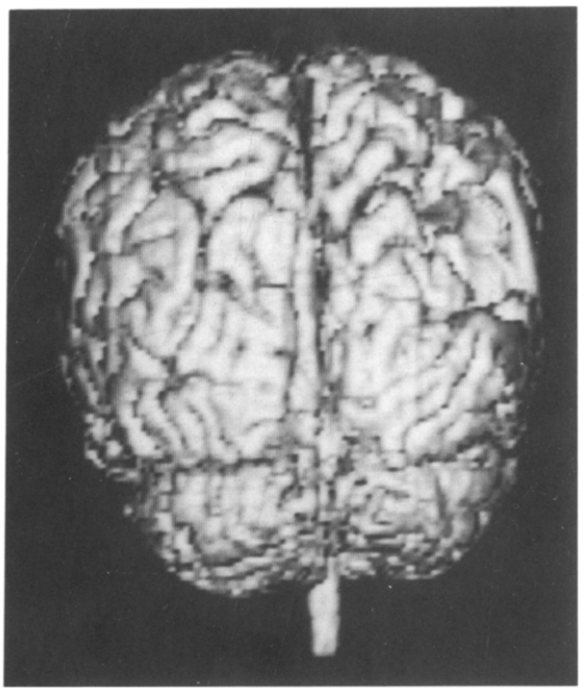

Fig. 6. Surface-based representation of the brain obtained from 128 MR slices by region growing and a morphological opening operation. Note the communication between the occipital horn of the lateral ventricular and subarachnoidal space.

Because of the flexibility of the model, the search may become computationally expensive. This optimization strategy is therefore practically limited to objects with a small number of generic constraints, such as smoothness, compactness, symmetry and homogeneity. Also, the search typically requires an initialization, for example in the form of a rough approximation of the contour to be found. This task requires a human-computer interface similar to the one needed for manual delineation.

Delineation of the left heart ventricle in SPECT and PET images using dynamic programming

Images of the perfusion (PET, SPECT) or the metabolism (PET) of the left ventricular wall have been used for the diagnosis of acute and chronic ischaemic heart disease, for the evaluation of therapeutic strategy and patient's prognosis. The gray values are approximately proportional to the tracer uptake and are normally highest for myocardial voxels. The absence of contrast in ischaemic or infarcted regions requires the use of a priori global shape knowledge of the left ventricle during segmentation.

The delineation algorithm is applied to a set of resliced radial images through the long axis, which is manually specified by the user. Initially, all the radial slices are

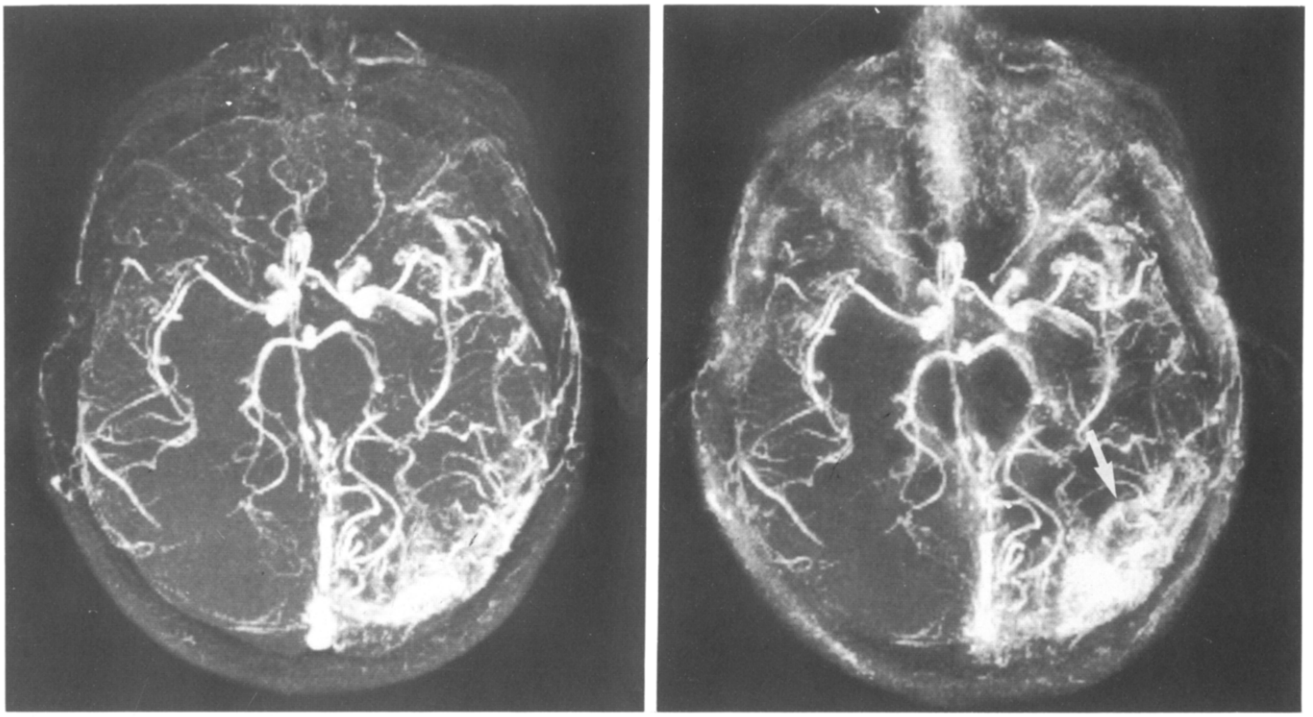

Fig. 7. (a) Maximum intensity projection (MIP) of original MRA. (b) MIP of filtered MRA with a morphological line detector. Black vessels become visible now.

summed, resulting in an average radial slice that is smoother and more uniform than the individual slices. A local maxima detector yields candidate center line points in this average slice. Using a least squares approximation, a piecewise ellipse is then fitted to the center line points. With dynamic programming, the endocardium and the epicardium of the left ventricle in all the radial slices are then found as smooth curves approximately parallel to the piecewise elliptical center line. Based on these contours, an improved parametric center line is calculated, which is then used in turn to find an improved endocardial and epicardial contour. The process typically requires two to five iterations. The base of the left ventricle is assumed to be planar. The delineation is completed by applying an iterative fitting algorithm to locate the basal plane. Figure 8a shows the result. More details of the delineation method can be found in [4,5].

From the epicardial and endocardial contour, a polar map (Fig. 8b) and corresponding diagnostic parameters

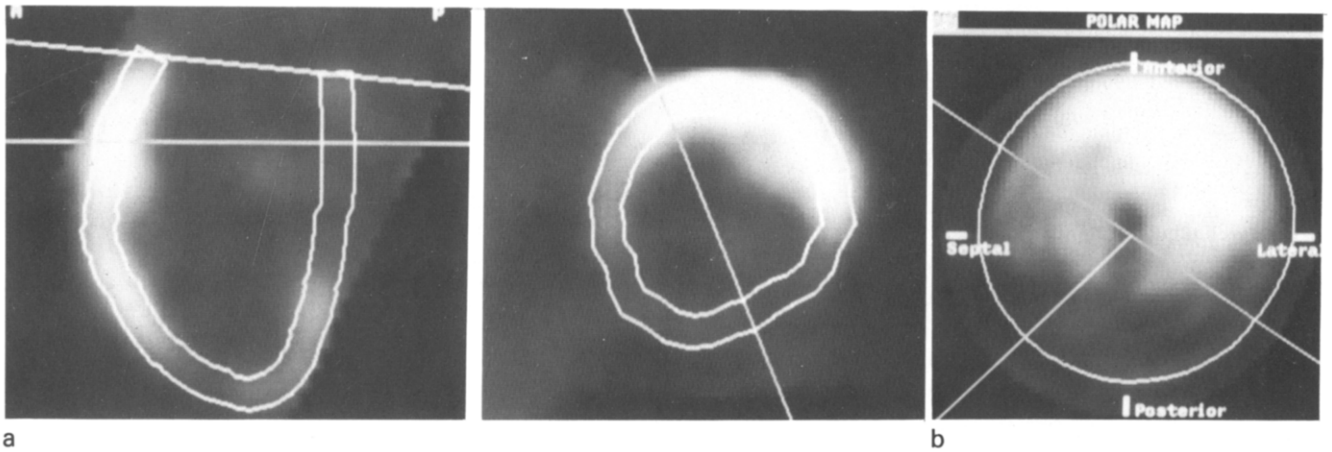

Fig. 8. (a) Endocardial and epicardial contours in a radial and axial SPECT slice of a patient injected with the tracer MIBI. (b) Corresponding polar map.

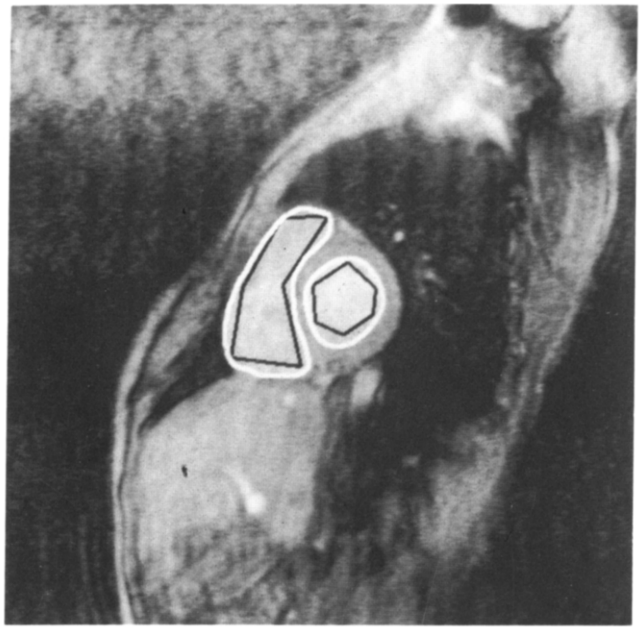

Fig. 9. Endocardial outline of the left and of the right heart ventricle in an MR slice. The contours were roughly indicated manually and further improved by the 'snake' algorithm. (Courtesy J. Bogaert).

are then calculated. Particularly, the extent and severity of myocardial perfusion defect is calculated by comparison to reference polar maps. The outlined ventricular wall can also be used to estimate the mass of the myocardial wall, the volume of the cavity, the stroke volume in gated studies and to estimate spill-over and recovery values. Dynamic series of PET polar maps can be analyzed to calculate the absolute value of flow and glucose metabolism.

The method was tested by simulations and by phantom measurements [5]. It has been successfully applied to more than 400 SPECT studies. Manual corrections of the delineation or of the position of the basal plane were necessary in only 15% of the cases. Most of the delineation inaccuracies occurred near infarcted regions close to relatively high background activity of the liver or the colon. The correct position of the basal plane is sometimes hard to define because no sharp edges are found near the base, which is probably due to motion of the heart.

Endocardial delineation in MRI using 'snakes'

Figure 9 shows the endocardial outline of the left and of the right heart ventricle in an MR slice. The contours were found by the 'snake' algorithm described in [6]. We use this method to calculate the enddiastolic and endsystolic volumes, ejection fraction and cardiac output from a series of consecutive slices.

The algorithm starts from an initial rough contour approximation entered by the user (Fig. 9). The contour is

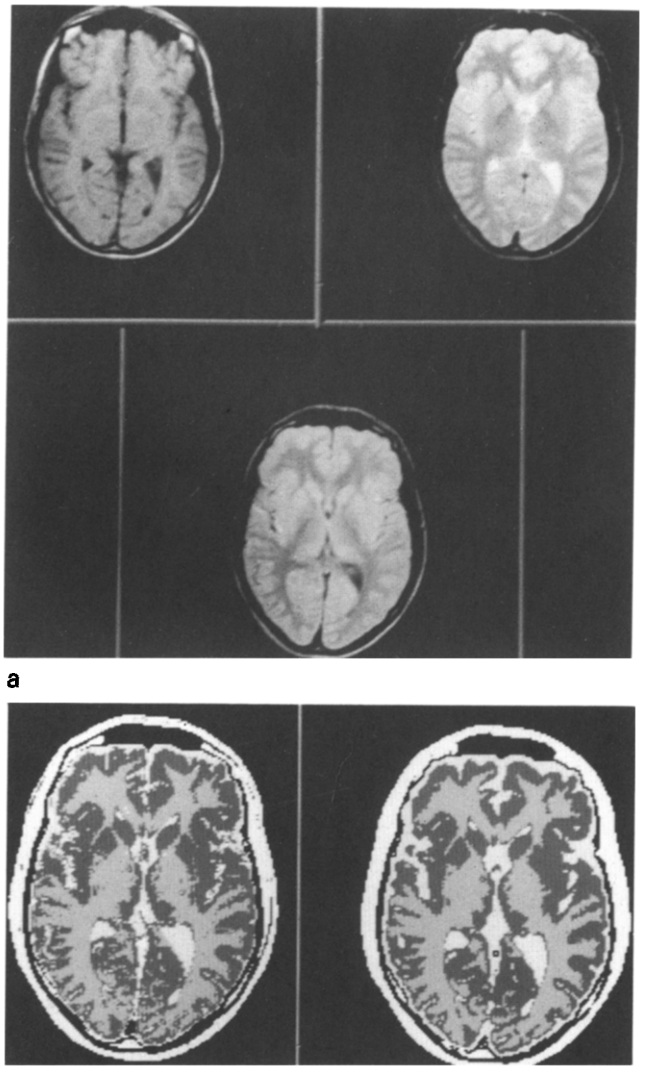

a

b

Fig. 10. (a) T1, T2 and ρ weighted MR image of the brain. (b) Result of segmentation. Note the improved performance of the right image as compared with the left, which was obtained without taking into account anatomical constraints.

then expanded by the optimization process until it sticks in a position of minimum energy.

The energy is a weighted function of different terms, such as the edge strength along the curve, the smoothness of the curve and the distance of the curve to important interactively defined points. As compared to the method of dynamic programming, used in the previous example, 'snakes' allow to use those global constraints whose energy cannot be calculated independently for different parts of the curve. For a more detailed comparison we refer to Ref. 7.

Soft tissue segmentation in MRI using stochastic relaxation

The 3D morphological filter described under 'low-level segmentation' uses only local properties for blood vessel segmentation. Optimization methods are con-

siderably slower than local filters but are suited to take global model knowledge, such as the continuity of the blood vessels, into account.

If the energy function is defined as the expected number of misclassified voxels, global continuity of blood vessels can be obtained by stochastic relaxation [1,8,9]. This optimization procedure iteratively changes the segmentation result and stochastically reduces the energy by eliminating relational inconsistencies, i.e. discontinuities.

We have also applied this method to MR brain tissue segmentation [8,9]. The algorithm uses a T1, T2 and ρ weighted image as the input data (Fig. 10a). The segmented structures are skin, bone, cerebrospinal fluid, gray and white matter. A priori geometric information has been used in the form of a number of rules that express anatomical incompatibilities between neighboring tissue types, e.g. skin must not be adjacent to white matter. A typical result is shown in Fig. 10b. Note the improved performance of the right image as compared with the left, which was obtained without the anatomical constraints. Despite this improvement, the image also shows that the result is not yet clinically useful. Further improvements can certainly be obtained by the use of a more complete anatomical model, such as a digital statistical brain atlas. However, such an atlas does not include all the pathological cases and it can therefore be expected that the clinical usefulness of this method will still be somewhat limited.

3. Discussion

We have discussed different applications of manual, low-level, and model-based segmentation. Low-level methods are popular because of their simplicity and speed. They are practically limited, however, to high-contrast images. Model-based segmentation methods are theoretically more powerful because they are able to employ global and semantic knowledge of structures to be segmented. They work well when the model can be expressed in terms of a few number of global constraints. However, in practice it turns out to be very difficult to express semantics such as anatomical knowledge in a complete and unambiguous way. For such complex models, other strategies may be more appropriate [7]. For example, if the knowledge about the object and its context is extensive and uncertain, heuristic procedures may be unavoidable. Solving problems by using such a large amount of domain-specific knowledge has led to the notion of knowledge systems or expert systems. The strategy to build an expert system is fundamentally different from optimization. Unlike optimization, expert systems reason about symbols extracted from the image data. In [10–12] an expert system is described for the automatic segmentation and interpretation of the coronary blood vessels in DSA images. However, due to its strong heuristic nature this method has limited clinical value. Generally, the number of clinical applications reduces with the level and extent of prior knowledge used by the segmentation algorithm.

Most problems of segmentation inaccuracies can be overcome by human interaction. Promising segmentation methods for complex images are therefore semi-automatic. They require manual intervention and guidance and consist of fast and accurate refinement techniques to complement the human operator.

4. Acknowledgements

This work has been supported by IBM Belgium (Academic Joint Study) and by the National Fund for Scientific Research, Belgium, under grant number FGWO 3.0115.92.

5. References

1 Vandermeulen D, Delaere D, Suetens P, Bosmans H, Marchal G. Local filtering and global optimisation methods for 3D magnetic resonance angiography (MRA) image enhancement. SPIE Visual Biomed Comput 1992; 1808: 274–288.

2 Bosmans H, Marchal G, Van Hecke P, Vandermeulen D, Suetens P. Magnetic resonance angiography: techniques, prospects and limitations. Frontiers Eur Radiol 1990; 7: 69–86.

3 Suetens P, Verbeeck R, Delaere D, Nuyts J, Bijnens B. Model-based image segmentation: methods and applications. Proceedings of the 3rd Conference on Artificial Intelligence in Medicine 1991: 3–24.

4 Nuyts J, Suetens P, Oosterlinck A, De Roo M, Mortelmans L. Delineation of ECT images using global constraints and dynamic programming. IEEE Trans Med Imaging 1991; 10: 489–498.

5 Nuyts J, Mortelmans L, Suetens P, Oosterlinck A, De Roo M. Model based quantification of myocardial perfusion images from SPECT. J Nucl Med 1989; 30: 1992–2001.

6 Daneels D, Van Campenhout D, Niblack W, Equitz W, Barber R, Bellon E, Fierens F. Interactive outlining: an improved approach using active contours. SPIE Storage Retrieval Image Video Data Bases 1993; 1908. In press.

7 Suetens P, Fua P, Hanson AJ. Computational strategies of object recognition. ACM Comput Surv 1992; 24: 5–61.

8 Verbeeck R, Vandermeulen D, Delaere D, Suetens P, Marchal G. Fuzzy voxel labeling of magnetic resonance images by global optimization. Proceedings of EUSIPCO-92 Signal Processing VI 1992; 3: 1453–1456.

9 Verbeeck R, Vandermeulen D, Berben L, Suetens P, Marchal G. Magnetic resonance voxel labeling based on Bayesian decision theory. SPIE Medi Imaging 1993; 1898. In press.

10 Suetens P, Smets C, Van de Werf F, Oosterlinck A. Recognition of the coronary blood vessels on angiograms using hierarchical model-based iconic search. Proceedings of IEEE CVPR 1989: 576–581.

11 Delaere D, Smets C, Suetens P, Marchal G, Van de Werf F. A knowledge-based system for the 3D reconstruction of blood vessels from two angiographic projections. J Med Biomed Eng Comp 1991; 29: 27–36.

12 Smets C, Van de Werf F, Suetens P, Oosterlinck A. An expert system for the labeling and 3D reconstruction of the coronary arteries from two projections. Int J Cardiac Imaging 1990; 5: 145–154.